JOURNAL OF GUIDANCE, CONTROL, AND DYNAMICS
Vol. 22, No. 4, July–August 1999

Dissipator Placement Design for Truss Structures via Balancing Theory

Chien-Chang Lin*
National Chung-Hsing University, Taichung 402, Taiwan, Republic of China
and
Huang-Nan Huang† and Fang-Bo Yeh‡
Tunghai University, Taichung 407, Taiwan, Republic of China

Application of a balancing theory to the placement of energy dissipators for truss structures is discussed. To apply the balancing theory, the equation of motion for a slightly damped truss structure is transformed into modal state-space representation, which is almost invariant under balanced realization. The ratio of future output energy to pass control input energy under state-space representation is chosen as the placement index to design the best placement of energy dissipators. Two types of placement indices are proposed: one is for a fixed initial condition, and the other is for worst-case design, i.e., considering all possible initial conditions. Various configurations with different dissipator placements are designed based on the placement indices. Numerical results show that these placement indices can be used as a good design criterion for the placement of linear-friction dissipators for truss structures with a global property.

I. Introduction

TRUSS structures are commonly used for antennas, transmission towers, and many critical components of equipment. Vibrations induced by wind, earthquakes, and other disturbances are important factors for design considerations for such structures. One means of reducing vibration is to provide sufficient damping for dissipation of energy. Passive damping is sought to alleviate the spillover phenomenon in those modes that are not included in the controller design. Inaudi et al.[1] investigated the damping effect of energy dissipative restraint (EDR) for the dynamic response of truss structures. They developed an equivalent linear model for design purposes and discussed three different configurations of the EDR placement for truss structures. However, which of these three configurations gives the best EDR placement is not discussed. In this paper, we present a placement index that can be used to indicate the level of damping effect provided by each type of configuration of EDR placement.

In general, there are three common methods for the placement of dissipators. The first method is to select the configuration with large modal damping. Its shortcoming is that only certain specified modes that are only applicable to the structure without mode-interactive damping effect can be considered. Hence, if some other modes are excited, such configurations may not provide more damping effect than the other types. The second method, as used by Zambrano et al.,[2] is to apply the modal strain energy first and then to select the configuration with a larger damping coefficient. This method has the same disadvantage as the first one. The third method is to select the configuration with a simple weighted average of the inverse of the damping ratio. Physically, the results represent the mean-square response of the structure to some white noise excitations. The difficulty of this method is how to choose suitable weightings such that the design configuration can provide more effective damping than others under different circumstances. Thus, it is necessary to develop a global design scheme to place the damper for truss to overcome the disadvantages of described methods. In this paper, a nonmodal-based method is developed to provide an overall damping effect for comparison of the amount of damping provided by different types of configurations. Our method is similar to the third method, but the weightings are chosen from the point of view of balancing theory, i.e., the relationship between input and output energy of the structure.

Many applications of balancing theory to the control of flexible structures have been studied to overcome the lack of proper scaling properties of the modal approach. The reader can refer to Gawronski[3] for more detailed information. Other studies[4–6] are concerned with the sensor and actuator locations for flexible structures using the modal and balanced coordinates. Gawronski and Lim[6] derived the root-mean-square law of the Hankel singular values to determine the actuator or sensor location in terms of both the system controllability and the system observability. The controllability and observability properties of flexible structures have been analyzed by many investigations.[5–12] Based on these controllability and observability properties, we can perform the balanced realization of flexible structure. Because there are some residual modes with lowest singular values of the joint gramian eliminated by the balancing theory in controller design, we would expect that the passive damping is sought to alleviate the spillover phenomenon. Hence, we consider the possibility of applying the balancing theory to design the passive damping for those residual modes. To the best of our knowledge, there is no direct application of the balancing theory to the damper placement problem of truss structures.

We first give a brief review of the controllability gramian, observability gramian, and Hankel singular values. The mathematical models for different system realizations of truss structures with dissipators are then presented. Thereafter, the index for the placement of energy dissipators is derived based on the relationship between Hankel singular values and global damping effect. Some numerical examples are discussed for evaluation and illustrative purposes.

II. Balancing of Finite Dimensional Systems

In this section, we give a brief review of the basic properties related to balancing of linear systems. Let G be a stable system governed by a differential equation of the form

$$G: \begin{aligned} \dot{\boldsymbol{x}}(t) &= \boldsymbol{A}\boldsymbol{x}(t) + \boldsymbol{B}\boldsymbol{u}(t) \\ \boldsymbol{y}(t) &= \boldsymbol{C}\boldsymbol{x}(t) \end{aligned} \tag{1}$$

where $\boldsymbol{x}(t) \in \boldsymbol{R}^n$, $\boldsymbol{u}(t) \in \boldsymbol{R}^m$, $\boldsymbol{y}(t) \in \boldsymbol{R}^p$, $\boldsymbol{A} \in \boldsymbol{R}^{n\times n}$, $\boldsymbol{B} \in \boldsymbol{R}^{n\times m}$, and $\boldsymbol{C} \in \boldsymbol{R}^{p\times n}$ are continuous real matrix-valued functions and $\boldsymbol{R}$ is a set of all real numbers.

Received 21 April 1998; revision received 2 December 1998; accepted for publication 7 December 1998.

*Professor, Department of Applied Mathematics. cclin@amath.nchu.edu.tw. Associate Fellow AIAA.

†Lecturer, Department of Mathematics; currently Graduate Student, Department of Applied Mathematics, National Chung-Hsing University, Taichung 402, Taiwan, Republic of China; nhuang@mail.thu.edu.tw.

‡Professor, Department of Mathematics; f.b.yeh@math.thu.edu.tw.

It is often convenient to assume that the system is relaxed in the infinitely remote pass, i.e., $\lim_{t\to-\infty} \boldsymbol{x}(t) = 0$. The triple of matrices $(\boldsymbol{A}, \boldsymbol{B}, \boldsymbol{C})$ is a realization of the system. Assuming this system is both controllable and observable, then the pair $(\boldsymbol{A}, \boldsymbol{B})$ is controllable and $(\boldsymbol{C}, \boldsymbol{A})$ is observable.

The controllability function $L_c(\boldsymbol{x}_0)$ and observability function of $L_0(\boldsymbol{x}_0)$ of the linear system (1) are defined as

$$L_c(\boldsymbol{x}_0) \triangleq \min_{\substack{\boldsymbol{u}\in L^2(-\infty,0)\\ \boldsymbol{x}(-\infty)=\boldsymbol{0},\, \boldsymbol{x}(0)=\boldsymbol{x}_0}} \frac{1}{2}\int_{-\infty}^{0} \boldsymbol{u}(t)^T\boldsymbol{u}(t)\,\mathrm{d}t$$

$$L_0(\boldsymbol{x}_0) \triangleq \frac{1}{2}\int_{0}^{\infty} \boldsymbol{y}(t)^T\boldsymbol{y}(t)\,\mathrm{d}t \tag{2}$$

where $\boldsymbol{x}(0) = \boldsymbol{x}_0$ and $\boldsymbol{u}(t) = \boldsymbol{0}$ for $t \geq 0$. These mean that $L_c(\boldsymbol{x}_0)$ is the minimum control input energy, which is used to drive the system state from rest $[\boldsymbol{x}(-\infty) = \boldsymbol{0}]$ to the current state $[\boldsymbol{x}(0) = \boldsymbol{x}_0]$, and that $L_0(\boldsymbol{x}_0)$ is the free output response energy from the state at $\boldsymbol{x}(0) = \boldsymbol{x}_0$ without any control input $[\boldsymbol{u}(t) = \boldsymbol{0},\ t \geq 0]$.

It is easy to verify that

$$L_c(\boldsymbol{x}_0) = \tfrac{1}{2}\boldsymbol{x}_0^T\boldsymbol{W}_c^{-1}\boldsymbol{x}_0, \qquad L_0(\boldsymbol{x}_0) = \tfrac{1}{2}\boldsymbol{x}_0^T\boldsymbol{W}_o\boldsymbol{x}_0 \tag{3}$$

where $\boldsymbol{W}_c$ and $\boldsymbol{W}_o$ are the system controllability and system observability gramians, respectively. They are the solutions of the following Lyapunov equations:

$$\boldsymbol{AW}_c + \boldsymbol{W}_c\boldsymbol{A}^T + \boldsymbol{BB}^T = 0, \qquad \boldsymbol{A}^T\boldsymbol{W}_o + \boldsymbol{W}_o\boldsymbol{A} + \boldsymbol{C}^T\boldsymbol{C} = 0 \tag{4}$$

and both matrices are positive definite for stable $\boldsymbol{A}$.

The Hankel singular value σ_i of the system is equal to the square root of the eigenvalue of matrix $\boldsymbol{W}_c\boldsymbol{W}_o$, and it is invariant under different representations of the system. The system's triple $(\boldsymbol{A}, \boldsymbol{B}, \boldsymbol{C})$ is balanced if its controllability and observability gramians are equal and diagonal as proposed by Moore[13]

$$\boldsymbol{W}_c = \boldsymbol{W}_o = \Gamma^2, \qquad \Gamma = \mathrm{diag}(\sigma_1, \ldots, \sigma_n)$$

$$\sigma_i \neq \sigma_j \quad \text{for} \quad i \neq j, \qquad \sigma_i > 0 \text{ for all } i \tag{5}$$

where σ_i is the ith Hankel singular value of the system. This realization is an ordered balanced realization if $\sigma_1 > \sigma_2 > \cdots > \sigma_n > 0$ to the conditions given in Eq. (5).

Any given representation $(\boldsymbol{A}, \boldsymbol{B}, \boldsymbol{C})$ of Eq. (1) can be transformed into balanced realization using the methods proposed by Glover.[14] Suppose the current state $\boldsymbol{x}(0)$ of a balanced system is partitioned as $\boldsymbol{x}_0 = [x_{01}, \ldots, x_{0n}]^T$, then the controllability and observability functions have the form

$$L_c(\boldsymbol{x}_0) = \frac{1}{2}\left[\frac{1}{\sigma_1}x_{01}^2 + \frac{1}{\sigma_2}x_{02}^2 + \cdots + \frac{1}{\sigma_n}x_{0n}^2\right]$$

$$L_o(\boldsymbol{x}_0) = \frac{1}{2}\left[\sigma_1 x_{01}^2 + \sigma_2 x_{02}^2 + \cdots + \sigma_n x_{0n}^2\right] \tag{6}$$

III. Truss Structures with EDR Elements

A truss structure (as shown in Fig. 1) in which some truss elements are embedded with EDR devices to providing damping to the structure as shown in Fig. 2 is considered. The detailed properties and hysteretic loop characteristics of EDR devices can be found in Ref. 1. Positions of EDR devices, as shown in Fig. 2a, are six candidate locations. We want to find the best locations for EDR devices to dissipate the vibration energy of the truss structure.

First, the mathematical model for truss structures with EDR devices is presented, and then the relationship between Hankel singular values and the structure parameters of damping ratios and natural frequencies are derived. Thereafter, the ratio of output response energy to the control input energy in balanced realization is chosen as the placement index for the design of EDR devices within the truss structure.

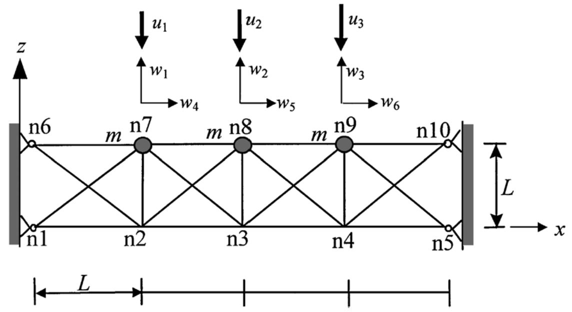

Fig. 1 Truss structure without EDR devices.

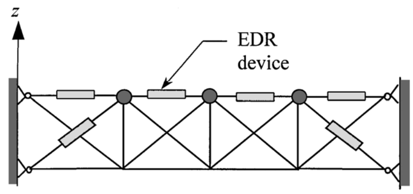

a) Configuration I

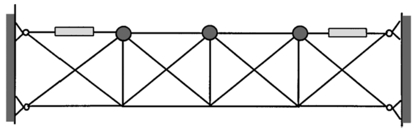

b) Configuration II

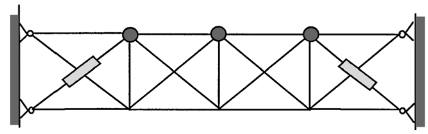

c) Configuration III

Fig. 2 Truss structure with EDR devices.

A. Mathematical Model

The motion of the structure about its initial configuration can be described by the following differential equations:

$$\boldsymbol{M}\ddot{\boldsymbol{w}}(t) + \boldsymbol{K}\boldsymbol{w}(t) + \sum_{i=1}^{N_e}\boldsymbol{L}_i^T\boldsymbol{f}_i(t) = \boldsymbol{L}_u\boldsymbol{u}(t)$$

$$\boldsymbol{w}(0) = \boldsymbol{w}_0, \qquad \dot{\boldsymbol{w}}(0) = \dot{\boldsymbol{w}}_0 \tag{7}$$

where the components of $\boldsymbol{w}(t)$ with dimension N are nodal displacements, $\boldsymbol{M}$ is the mass matrix, $\boldsymbol{K}$ is the stiffness matrix without the effect of EDR devices, $\boldsymbol{L}_u$ is the transformation for excitation $\boldsymbol{u}(t)$ with dimension m, $\boldsymbol{f}_i(t)$ is the force in the ith rod containing an EDR device, $\boldsymbol{L}_i$ is the appropriate force transformation, and N_e is the number of EDR devices. The force in the ith damper can be expressed as

$$\boldsymbol{f}_i(t) = k_m^{(i)}\Delta_i(t) + \boldsymbol{g}\left[\Delta_i(t), l_i(t), z_i(t), k_h^{(i)}, \lambda_i\right] \tag{8}$$

where $k_m^{(i)}$, $k_h^{(i)}$, and λ_i are the parameters of the ith EDR, $z_i(t)$ is the previous deformation (memory) of the ith EDR, $l_i(t) = \mathrm{sign}(\Delta_i\dot{\Delta}_i)$, and Δ_i is the element deformation of the ith element given by

$$\Delta_i(t) = \boldsymbol{L}_i\boldsymbol{w}(t) \tag{9}$$

and $\boldsymbol{g}[\Delta_i(t), l_i(t), z_i(t), k_h^{(i)}, \lambda_i]$ is the damping contribution from the ith EDR, which has the form[1]

$$\boldsymbol{g}(\Delta, l, z, k_h, \lambda) = \begin{cases} k_h\Delta & \text{if } l = 1 \text{ and } |\Delta| > |z/\bar{\lambda}| \\ k_h[\lambda\Delta - z(\lambda+1)] & \text{if } l = 1 \text{ and } |z| < |\Delta| < |z/\bar{\lambda}| \\ -k_h\Delta & \text{if } l = -1 \text{ and } |\Delta| < |z\bar{\lambda}| \\ k_h[\lambda\Delta - z(\lambda-1)] & \text{if } l = -1 \text{ and } |z| > |\Delta| > |z\bar{\lambda}| \end{cases} \tag{10}$$

where $\bar{\lambda} = (\lambda - 1)/(\lambda + 1)$. By defining

$$\tilde{\boldsymbol{K}} = \boldsymbol{K} + \sum_{i=1}^{N_e} k_m^{(i)} \boldsymbol{L}_i^T \boldsymbol{L}_i$$

Eq. (7) can be written as

$$\boldsymbol{M}\ddot{\boldsymbol{w}}(t) + \tilde{\boldsymbol{K}}\boldsymbol{w}(t) + \sum_{i=1}^{N_e} \boldsymbol{L}_i^T \boldsymbol{g}\left[\Delta_i(t), l_i(t), z_i(t), k_h^{(i)}, \lambda_i\right] = \boldsymbol{L}_u \boldsymbol{u}(t) \tag{11}$$

Through the harmonic linearization technique, Inaudi and Kelly[15] developed an equivalent linear element for EDR of the form

$$\bar{g}(t) = k_e \Delta(t) + c_e \dot{\Delta}(t) \tag{12}$$

to replace the generally nonlinear component $\boldsymbol{g}[\Delta_i(t), l_i(t), z_i(t), k_h^{(i)}, \lambda_i]$ in Eq. (10); the equivalent parameters are $k_e = k_h \rho_k(\lambda)$ and $c_e = (2k_h/\pi\omega_1)\rho_c(\lambda)$, where ω_1 is the fundamental frequency of the element with EDR in the truss structure and the functions $\rho_k(\lambda)$ and $\rho_c(\lambda)$ are given by[15]

$$\rho_k(\lambda) = (1/\pi)\left[(1+\lambda)\cos^{-1}\bar{\lambda} - 2\bar{\lambda}\sqrt{\bar{\lambda}}\right], \qquad \rho_c(\lambda) = \bar{\lambda}$$

Therefore, the corresponding linearized differential equation of Eq. (11) is

$$\boldsymbol{M}\ddot{\boldsymbol{w}}(t) + \sum_{i=1}^{N_e} c_e^{(i)} \boldsymbol{L}_i^T \boldsymbol{L}_i \dot{\boldsymbol{w}}(t) + \left(\tilde{\boldsymbol{K}} + \sum_{i=1}^{N_e} k_e^{(i)} \boldsymbol{L}_i^T \boldsymbol{L}_i\right)\boldsymbol{w}(t) = \boldsymbol{L}_u \boldsymbol{u}(t) \tag{13}$$

The output response $\boldsymbol{y}(t)$ can be represented by the system's output matrix $\boldsymbol{C}_q$ and $\boldsymbol{C}_v$ as

$$\boldsymbol{y}(t) = \boldsymbol{C}_q \boldsymbol{w}(t) + \boldsymbol{C}_v \dot{\boldsymbol{w}}(t)$$

B. State-Space Representation

If φ_j is the jth modal function for the natural frequencies ω_j of the undamped system,

$$\omega_j^2 \boldsymbol{M}\varphi_j = \left(\tilde{\boldsymbol{K}} + \sum_{i=1}^{N_e} k_e^{(i)} \boldsymbol{L}_i^T \boldsymbol{L}_i\right)\varphi_j$$

$$\varphi_i^T \boldsymbol{M} \varphi_j = \delta_{ij} \qquad j = 1, 2, \ldots, N \tag{14}$$

or in matrix form

$$\boldsymbol{M}\boldsymbol{\Phi}\boldsymbol{\Omega}^2 = \left(\tilde{\boldsymbol{K}} + \sum_{i=1}^{N_e} k_e^{(i)} \boldsymbol{L}_i^T \boldsymbol{L}_i\right)\boldsymbol{\Phi}, \qquad \boldsymbol{\Phi}^T \boldsymbol{M} \boldsymbol{\Phi} = \boldsymbol{I} \tag{15}$$

The modal coordinates $\boldsymbol{q}(t)$ can be represented as

$$\boldsymbol{w}(t) = \boldsymbol{\Phi}\boldsymbol{q}(t) \tag{16}$$

After incorporating the orthogonal property of the modal matrix $\boldsymbol{\Phi} = [\varphi_1, \ldots, \varphi_N]$, the equivalent linear system for Eq. (13) can be written as

$$\ddot{\boldsymbol{q}}(t) + \sum_{i=1}^{N_e} c_e^{(i)} \boldsymbol{\Phi}^T \boldsymbol{L}_i^T \boldsymbol{L}_i \boldsymbol{\Phi} \dot{\boldsymbol{q}}(t) + \boldsymbol{\Omega}^2 \boldsymbol{q}(t) = \boldsymbol{\Phi}^T \boldsymbol{L}_u \boldsymbol{u}(t) \tag{17}$$

where $\boldsymbol{\Omega}$ is a diagonal matrix with diagonal elements ω_j. With the state variable $\boldsymbol{x}^T = [\boldsymbol{q}^T, \dot{\boldsymbol{q}}^T]$, we obtain the following state-space realization $(\boldsymbol{A}, \boldsymbol{B}, \boldsymbol{C})$ of appropriate dimensions $(n = 2N)$:

$$\boldsymbol{A} = \begin{bmatrix} \boldsymbol{0} & \boldsymbol{I} \\ -\boldsymbol{\Omega}^2 & -2\boldsymbol{Z}\boldsymbol{\Omega} \end{bmatrix}, \qquad \boldsymbol{B} = \begin{bmatrix} \boldsymbol{0} \\ \boldsymbol{\Phi}^T \boldsymbol{L}_u \end{bmatrix}$$

$$\boldsymbol{C} = [\boldsymbol{C}_q \boldsymbol{\Phi} \quad \boldsymbol{C}_v \boldsymbol{\Phi}] \tag{18}$$

in which $\boldsymbol{Z}$ is the modal damping matrix satisfying

$$2\boldsymbol{Z}\boldsymbol{\Omega} = \sum_{i=1}^{N_e} c_e^{(i)} \boldsymbol{\Phi}^T \boldsymbol{L}_i^T \boldsymbol{L}_i \boldsymbol{\Phi} \tag{19}$$

Neglecting the interaction between modal coordinates, the uncoupled damping matrix $\boldsymbol{Z}$ becomes

$$\boldsymbol{Z} = \mathrm{diag}(\zeta_j), \qquad \zeta_j = \frac{1}{\pi\omega_j^2} \sum_{i=1}^{N_e} k_h^{(i)} \rho_c(\gamma_i) \boldsymbol{\varphi}_j^T \boldsymbol{L}_i^T \boldsymbol{L}_i \boldsymbol{\varphi}_j$$

$$j = 1, 2, \ldots, N \tag{20}$$

C. Modal State-Space Representation

The state-space realization is constructed based on the modal analysis technique. Equation (17) is transformed into modal state-space representation by the matrix $\boldsymbol{T}$, which consists of $\boldsymbol{T}_j$

$$\boldsymbol{T}_j = \begin{bmatrix} 1 & 0 \\ \zeta_j & 1/\omega_j \end{bmatrix}$$

for the jth mode in which $j = 1, 2, \ldots, N$. This realization is obtained as a triple $(\boldsymbol{A}_m, \boldsymbol{B}_m, \boldsymbol{C}_m)$ of the form

$$\boldsymbol{A}_m = \mathrm{diag}(\boldsymbol{A}_1, \boldsymbol{A}_2, \ldots, \boldsymbol{A}_N), \qquad \boldsymbol{B}_m^T = \left[\boldsymbol{B}_1^T, \boldsymbol{B}_2^T, \ldots, \boldsymbol{B}_N^T\right]$$

$$\boldsymbol{C}_m = [\boldsymbol{C}_1, \boldsymbol{C}_2, \ldots, \boldsymbol{C}_N] \tag{21}$$

where

$$\boldsymbol{A}_j = \begin{bmatrix} -\zeta_j\omega_j & \omega_j \\ -\omega_j & -\zeta_j\omega_j \end{bmatrix}, \qquad \boldsymbol{B}_j = \begin{bmatrix} \boldsymbol{0} \\ \boldsymbol{b}_j \end{bmatrix}, \qquad \boldsymbol{C}_j = [\boldsymbol{c}_{qj} \quad \boldsymbol{c}_{vj}]$$

$$j = 1, 2, \ldots, N$$

and $\boldsymbol{b}_j = \boldsymbol{\varphi}_j^T \boldsymbol{L}_u/\omega_j$, $\boldsymbol{c}_{qj} = (\boldsymbol{C}_q - \zeta_j\omega_j\boldsymbol{C}_v)\boldsymbol{\varphi}_j$, $\boldsymbol{c}_{vj} = \omega_j \boldsymbol{C}_v \boldsymbol{\varphi}_j$. It is noted that the term $-\zeta_j^2\omega_j$ in the block (2, 1) of matrix $\boldsymbol{A}_j$ has been neglected. The component of the state vector corresponding to the jth block is $\boldsymbol{x}_{mj} = [q_j \quad q_{0j}]^T$, where q_j is the jth modal displacement and $q_{0j} = \zeta_j q_j + \dot{q}_j/\omega_j$, where $\dot{q}_j$ is the jth modal velocity.

D. Placement Index

The input–output assignment in the present problem is fixed to investigate the energy damping effects of different placements of EDR devices. Two important features of a flexible structure, as discussed in Ref. 6, are used in the present analysis. First, the states in modal coordinate are approximately orthogonal. Second, the state matrix $\boldsymbol{A}$ in the balanced coordinates is diagonally dominant. To identify the overall damping effect, we consider the equation of motion given by Eq. (7) for the system. To validate the damping effects of different configurations of a flexible structure, we select the current state of the system to be invariant for various configurations. For a flexible structure with proper damping, the structure should have spent more past input energy and exhibit less output energy. Therefore, a placement index $\gamma(\boldsymbol{x}_0)$ may be defined as

$$\gamma(\boldsymbol{x}_0) = \frac{L_o(\boldsymbol{x}_0)}{L_c(\boldsymbol{x}_0)} = \frac{\boldsymbol{x}_0^T \boldsymbol{W}_o \boldsymbol{x}_0}{\boldsymbol{x}_0^T \boldsymbol{W}_c^{-1} \boldsymbol{x}_0} = \sum_{i=1}^{n} \sigma_i x_{0i}^2 \Bigg/ \sum_{i=1}^{n} \frac{1}{\sigma_i} x_{0i}^2 \tag{22}$$

where x_{0i} is the corresponding component of the current state $\boldsymbol{x}_0$ in balanced representation. Before applying this index to design our problem, we would like to understand the relationship between the placement index and the modal damping coefficients.

Theoretically, there is no explicit relation between this index $\gamma(\boldsymbol{x}_0)$ and the overall system damping; however, the index $\gamma(\boldsymbol{x}_0)$ can be related to the summarized effect of an individual modal damping ratio and frequency whenever a small system damping is assumed. On the assumption of a small damping such that $\zeta \ll 1$ [$\zeta = \max(\zeta_j)$, $j = 1, 2, \ldots, N$], the balanced and modal state-space representations are closely related.[6,7] The corresponding $\boldsymbol{W}_c$ and $\boldsymbol{W}_o$ are

$$\boldsymbol{W}_c \cong \mathrm{diag}(w_{cj}\boldsymbol{I}_2), \qquad \boldsymbol{W}_o \cong \mathrm{diag}(w_{oj}\boldsymbol{I}_2)$$

$$j = 1, 2, \ldots, N \tag{23}$$

where $w_{cj} = \boldsymbol{b}_j\boldsymbol{b}_j^T/4\zeta_j\omega_j$, $w_{oj} = (\boldsymbol{c}_{qj}^T\boldsymbol{c}_{qj} + \boldsymbol{c}_{vj}^T\boldsymbol{c}_{vj})/4\zeta_j\omega_j$, and $\boldsymbol{I}_2$ is the 2×2 identity matrix. Their product is also diagonally dominant. Thus, the Hankel singular values are given by

$$\sigma_j \cong \sqrt{w_{cj} w_{oj}} = \sqrt{\frac{\boldsymbol{b}_j\boldsymbol{b}_j^T\left(\boldsymbol{c}_{qj}^T\boldsymbol{c}_{qj} + \boldsymbol{c}_{vj}^T\boldsymbol{c}_{vj}\right)}{16\zeta_j^2\omega_j^2}} \tag{24}$$

Assuming that the modal matrix $\boldsymbol{A}$ is almost the same for all different configurations, one can obtain the placement index $\gamma(\boldsymbol{x}_0)$ as follows:

$$\gamma(\boldsymbol{x}_0) \cong \sum_{j=1}^{N} \frac{\boldsymbol{c}_{qj}^T\boldsymbol{c}_{qj} + \boldsymbol{c}_{vj}^T\boldsymbol{c}_{vj}}{\zeta_j\omega_j}\left[q_j^2(0) + q_{0j}^2(0)\right] \Bigg/ 16\sum_{j=1}^{N} \frac{\zeta_j\omega_j}{\boldsymbol{b}_j\boldsymbol{b}_j^T}\left[q_j^2(0) + q_{0j}^2(0)\right] \tag{25}$$

From Eq. (25), the values of the terms $q_j^2(0) + q_{0j}^2(0)$ can be considered as the transformed weighting of the jth natural mode. If equal weightings are selected, i.e., $q_j^2(0) + q_{0j}^2 = 1/N$, then the index γ becomes

$$\gamma \cong \sum_{j=1}^{N} \frac{\boldsymbol{c}_{qj}^T\boldsymbol{c}_{qj} + \boldsymbol{c}_{vj}^T\boldsymbol{c}_{vj}}{\zeta_j\omega_j} \Bigg/ 16\sum_{j=1}^{N} \frac{\zeta_j\omega_j}{\boldsymbol{b}_j\boldsymbol{b}_j^T} \tag{26}$$

Typically, if the placement of an EDR device can produce more damping, the placement index is smaller. Therefore, this index can be used to indicate as to whether a selected placement is good or not. The placement index given in Eq. (26) is similar to the weighted average of the inverse of the damping ratio. the first vibration mode. Alternatively, we can choose a number of initial conditions $\boldsymbol{x}_0$, in which we are practically more interested, then choose the configuration with smallest placement index.

E. General Formulation

Now, we want to extend the preceding discussion to a more general system. Consider a general linear system G

$$\dot{\boldsymbol{x}} = \boldsymbol{A}(d_i)\boldsymbol{x} + \boldsymbol{B}\boldsymbol{u}, \qquad \boldsymbol{x}(0) = \boldsymbol{x}_0 \qquad i = 1, 2, \ldots, N_T$$
$$\boldsymbol{y} = \boldsymbol{C}\boldsymbol{x} \tag{27}$$

where $\boldsymbol{u}$ is the external force, $\boldsymbol{y}$ is the sensor measurement, $\boldsymbol{x} = [\boldsymbol{w} \;\; \dot{\boldsymbol{w}}]^T$ is the state vector, and d_i are indicator functions; here each d_i is used to denote whether the dissipator is placed on the ith truss or not ($d_i = 1$ or 0) satisfying the condition

$$\sum_{i=1}^{N_T} d_i = N_e$$

in which N_T is the total number of the truss elements. The modal parameters of the truss structure are determined by $\boldsymbol{A}$, which in turn is determined by the indicator functions d_i of the dissipators; $\boldsymbol{B}$ is determined by the locations where the external force $\boldsymbol{u}$ is applied; and $\boldsymbol{C}$ is determined by the locations where the deflection of the truss is most concerned and is to be measured.

The mathematical model for our truss structure, i.e., Eq. (13), can also be expressed in this framework with the following coefficient matrices:

$$\boldsymbol{A}(\boldsymbol{d}) = \begin{bmatrix} \boldsymbol{0} & \boldsymbol{I} \\ -\boldsymbol{M}^{-1}\displaystyle\sum_{i=1}^{N_T} d_i c_i^{(i)}\boldsymbol{L}_i^T\boldsymbol{L}_i & -\boldsymbol{M}^{-1}\left(\boldsymbol{K} + \displaystyle\sum_{i=1}^{N_T} d_i\left(k_m^{(i)} + k_e^{(i)}\right)\boldsymbol{L}_i^T\boldsymbol{L}_i\right) \end{bmatrix}, \qquad \boldsymbol{B} = \begin{bmatrix} \boldsymbol{0} \\ \boldsymbol{L}_u \end{bmatrix}, \qquad \boldsymbol{C} = [\boldsymbol{C}_q \quad \boldsymbol{C}_v]$$

For the flexible structure with moderate damping, in general, from the input–output energy point of view, we can apply the same placement index to help make configuration selections. The computational algorithm for this purpose is summarized as follows.

1) Compute the mass matrix $\boldsymbol{M}$ and stiffness matrix $\tilde{\boldsymbol{K}}$ with dimension N for the structure.

2) Set up all possible configurations and the maximum allowable number of EDR devices N_e.

3) Calculate the modal matrix $\boldsymbol{\Phi}$, damping matrix $\boldsymbol{Z}$, and natural frequencies ω_j; then assemble the matrix $\boldsymbol{A}$ and select proper $\boldsymbol{L}_u$ and desired output signals to compute $\boldsymbol{A}$, $\boldsymbol{B}$, and $\boldsymbol{C}$ according to Eq. (18).

4) Decide the initial condition $\boldsymbol{w}_0$ of interest and the corresponding $\boldsymbol{x}_0$.

5) Compute the matrices $\boldsymbol{W}_c$ and $\boldsymbol{W}_o$ using Eq. (4), and then calculate Hankel singular values σ_i, $i = 1, 2, \ldots, 2N$.

6) Compute the placement index $\gamma(\boldsymbol{x}_0)$ for each configuration by Eq. (22).

7) Decide on the best configuration with the smallest $\gamma(\boldsymbol{x}_0)$.

Inasmuch as the proposed placement index depends on the initial condition $\boldsymbol{x}_0$, for each special arrangement we require evaluating the index and checking whether it is small for all possible initial conditions. This is very inconvenient in real applications. A remedy is to consider the worst-case γ^*

$$\gamma^* = \max_{x_0} \gamma(\boldsymbol{x}_0) = \max_{x_0} \frac{\boldsymbol{x}_0^T\boldsymbol{W}_o\boldsymbol{x}_0}{\boldsymbol{x}_0^T\boldsymbol{W}_c^{-1}\boldsymbol{x}_0}$$

It can be shown that γ^* is indeed the square of the largest Hankel singular value, i.e., $\gamma^* = \sigma_1^2$. Hence, γ^* can serve as a worst-case design index. Therefore, for any given constant c, if we know $\gamma^* < c$, then we must have $\gamma(\boldsymbol{x}_0) < c$ for all possible $\boldsymbol{x}_0$. Although the worst-case design provides a more convenient way to decide the best configuration, it seems too conservative. At the same time, for a small damping system, by use of Eq. (24) σ_1 is approximately related to the first damping coefficient ζ_1. Thus, the worst-case strategy of selecting the dissipators arrangement is highly dependent on the first vibration mode.

where $\boldsymbol{d} = [d_1 \;\; \cdots \;\; d_{N_e}]^T$ is defined as an indicator vector.

The damping efficiency of dissipators depends on 1) where it locates ($\boldsymbol{d}_i$), 2) where the external force applies ($\boldsymbol{B}$), 3) how the external force is changing with time t [$\boldsymbol{u}(t)$], 4) where the location of the truss is concerned ($\boldsymbol{C}$), and 5) the initial condition ($\boldsymbol{x}_0$).

The following design problem is considered: Given physically motivated $\boldsymbol{B}$ and $\boldsymbol{C}$, propose a design criterion to find the best arrangement $\boldsymbol{d}$ of the dissipators with a total number less or equal to N_e under the action of all possible $\boldsymbol{u}(t)$ and under all possible deflections $\boldsymbol{x}_0$.

First, we can apply the balancing theory to solve this problem. Choose the Hankel norm (the largest Hankel singular value) as our placement index, i.e.,

$$\gamma(\boldsymbol{d}) = \|G\|_H^2 = \sup_{x_0} \frac{L_o(\boldsymbol{x}_0)}{L_c(\boldsymbol{x}_0)} = \sup_{x_0} \frac{\boldsymbol{x}_0^T\boldsymbol{W}_o(\boldsymbol{d})\boldsymbol{x}_0}{\boldsymbol{x}_0^T\boldsymbol{W}_c(\boldsymbol{d})^{-1}\boldsymbol{x}_0} = \sigma_1^2(\boldsymbol{d}) \tag{28}$$

where $\sigma_1(\boldsymbol{d})$ is the largest singular value of the matrix $\boldsymbol{W}_c(\boldsymbol{d})\boldsymbol{W}_o(\boldsymbol{d})$ and $\boldsymbol{W}_c(\boldsymbol{d})$ and $\boldsymbol{W}_o(\boldsymbol{d})$ are the solutions of the following equations:

$$\boldsymbol{A}(\boldsymbol{d})\boldsymbol{W}_c(\boldsymbol{d}) + \boldsymbol{W}_c(\boldsymbol{d})\boldsymbol{A}(\boldsymbol{d})^T + \boldsymbol{B}\boldsymbol{B}^T = 0$$
$$\boldsymbol{A}(\boldsymbol{d})^T\boldsymbol{W}_o(\boldsymbol{d}) + \boldsymbol{W}_o(\boldsymbol{d})\boldsymbol{A}(\boldsymbol{d}) + \boldsymbol{C}^T\boldsymbol{C} = 0 \tag{29}$$

Let D be the set of all possible candidates, i.e.,

$$D = \left\{\boldsymbol{d} = \left[d_1 \;\; \cdots \;\; d_{N_T}\right]^T \,\middle|\, d_1 + \cdots + d_{N_T} \le N_e\right\}$$

The best configuration in D is chosen to be the one that gives the smallest γ. If there exist more than one $\boldsymbol{d}$, then we choose the one that gives the smaller σ_2. We apply this procedure to all similar cases and decide which one is the best choice. Note that because the total number of Hankel singular values is $2N$, which is large than N_T and N_e in general, the possibility for any two different configurations to have all of the same Hankel singular values is extremely low.

On the other hand, if we are more concerned about the effect of the external disturbances, noises, and uncertainties on the truss structure, the H_∞ criterion is adopted to design the dissipator placement having a certain robust property. In this case, we choose the placement index to be the ratio of the total output energy to the total input energy, i.e.,

$$\gamma(\boldsymbol{d}) = \|G\|_\infty^2 = \sup_{x_0} \frac{\|\boldsymbol{y}\|_2^2}{\|\boldsymbol{u}\|_2^2} = \sup_{x_0} \frac{\int_0^\infty \boldsymbol{y}(t)^T \boldsymbol{y}(t)\, \mathrm{d}t}{\int_0^\infty \boldsymbol{u}(t)^T \boldsymbol{u}(t)\, \mathrm{d}t} \tag{30}$$

The smaller this index, the more damping the dissipators can provide. If more than two configurations have the same value of the index, there is no obvious method to check which one is more suitable. Hence, we will not apply this approach to our design problem later on.

IV. Results and Discussions

A. Verification Test

The example given in Ref. 1 is used to test the design idea. The basic layout of the truss structure without EDR devices is shown in Fig. 1. Three configurations containing EDR devices (configurations I, II, and III) shown in Fig. 2 are considered for the verification test. The mass of the structure is assumed to be lumped at the nodes of the top chord of equal magnitude m. The area A and Young's modulus E are the same for each truss element of length L or $(\sqrt{2})L$ with or without EDR devices. The parameters k_m and k_h of the embedded EDR devices are selected to be EA/L and $0.25EA/L$ or $EA/(\sqrt{2})L$ and $0.25EA/(\sqrt{2})L$ for each truss element of length L or $(\sqrt{2})L$, respectively, such that the same stiffness matrix $\tilde{\boldsymbol{K}}$ is obtained for different configurations.

Choosing $EA/mL = 1000\ \mathrm{s}^{-2}$, we obtain the modal matrix and natural frequencies for the truss structure as shown in Fig. 1 but without embedded EDR devices as follows:

$$\boldsymbol{\Phi} = \begin{bmatrix} -0.4700 & -0.5715 & -0.4124 & 0.5278 & 0.0229 & 0.0580 \\ -0.7343 & 0.0000 & 0.0000 & -0.6606 & 0.1562 & 0.0000 \\ -0.4700 & 0.5715 & 0.4124 & 0.5278 & 0.0229 & -0.0580 \\ 0.0976 & -0.2519 & 0.4207 & 0.0566 & 0.6980 & 0.5094 \\ 0.0000 & -0.4690 & 0.5530 & 0.0000 & 0.0000 & -0.6886 \\ -0.0976 & -0.2519 & 0.4207 & -0.0566 & -0.6980 & 0.5094 \end{bmatrix}$$

$$\omega_1 = 17.24, \qquad \omega_2 = 30.31, \qquad \omega_3 = 32.86$$

$$\omega_4 = 38.85, \qquad \omega_5 = 51.11, \qquad \omega_6 = 63.32$$

where ω is in radians per second and the columns of $\boldsymbol{\Phi}$ are the mode shapes normalized to have unit amplitude. The corresponding modal damping ratios and the first six natural frequencies for different configurations are summarized in Table 1.

Because the damping coefficients for these three configurations are much smaller than unity, we use the modal state-space realization to represent the dynamics of the system with initial conditions $\boldsymbol{w}(0) = \boldsymbol{0}$ and $\dot{\boldsymbol{w}}(0) = 121.9\varphi_1$ cm/s, which are the same as used in Ref. 1. Three control input signals, $u_1(t)$, $u_2(t)$, and $u_3(t)$, and six output signals, $w_i(t)$, $i = 1, 2, \ldots, 6$, are used to construct the realization $(\boldsymbol{A_m}, \boldsymbol{B_m}, \boldsymbol{C_m})$. Then, the output matrix $\boldsymbol{C}$ consists of two identity submatrices $\boldsymbol{C}_q$ and $\boldsymbol{C}_v$ of dimensions six. They reflect the full information of the modal states $\boldsymbol{x_m}(t)$. Thus, the Hankel singular values and the placement indices are evaluated by Eqs. (24) and (25), respectively, and listed in Table 2. To verify the effectiveness of the placement index, configuration I with six EDR devices can be selected as a design reference. From Table 2, because the placement indices γ and $\gamma^* = \sigma_1^2$ of configuration III is smaller than those of configuration II and closer to configuration I, configuration III is a better choice than configuration II with this initial condition. Simultaneously, we observed from Table 1 that the damping coefficients in the third, fifth, and sixth modes of configuration III are very close to zero, which means that this configuration has little capability to damp out the vibrations corresponding to the third, fifth, and sixth modes.

Table 1 Natural frequencies and damping ratios for different configurations of truss structure

Configuration	Mode	1	2	3	4	5	6
I	ω_i	17.64	31.40	33.56	39.17	53.43	66.23
	ζ_i	0.0297	0.0407	0.0317	0.0103	0.0573	0.0574
II	ω_i	17.30	30.48	33.44	38.85	52.09	66.75
	ζ_i	0.0041	0.0059	0.0240	0.0002	0.0251	0.0092
III	ω_i	17.52	31.12	32.86	39.16	51.49	63.51
	ζ_i	0.0206	0.0339	0.0000	0.0104	0.0101	0.0041

Table 2 Hankel singular values and placement indices for different output matrices

Configuration	σ_1	σ_2	σ_3	σ_4	σ_5	σ_6	γ
			$\boldsymbol{C}_q$, $\boldsymbol{C}_v$ selected as identity matrices				
I	2.8864	2.3111	1.7826	4.9247	0.7875	0.5965	69.807
II	7.7800	6.0711	2.2530	35.313	1.2271	1.4761	3663.6
III	3.4658	2.4438	148.61	4.9000	1.9629	2.3567	144.28
			$\boldsymbol{C}_q$ identity matrix and $\boldsymbol{C}_v$ zero matrix				
I	0.6876	0.4124	0.3077	0.7868	0.1077	0.0733	0.2235
II	1.8691	1.0995	0.3896	5.6646	0.1700	0.1849	12.206
III	0.8277	0.4381	25.919	0.7830	0.2735	0.2957	0.4694

To understand the effect of initial condition on the placement index, we try another initial condition $\boldsymbol{w}(0) = \boldsymbol{0}$ and $\dot{\boldsymbol{w}}(0) = 121.9\varphi_3$ cm/s, then the computed placement indices for these three configurations are 10.0981, 25.7675, and 4.8773×10^8, respectively. Under this condition, configuration II is a better choice.

Because the Hankel singular value of the structure is computed as a function of system output matrix $\boldsymbol{C}$ through Eq. (24), the placement indices are also affected. Table 2 also gives the values of placement indices for these three configurations with another output matrix $\boldsymbol{C}$, which consists of two submatrices $\boldsymbol{C}_q$ and $\boldsymbol{C}_v$ as an identity matrix and a zero matrix of dimensions six, respectively. Although the Hankel singular values and the placement indices given in Table 2 are different for the two types of output matrices, the trends of variations between the three configurations are similar.

This verification test reveals that the placement index can be used to indicate the quantity of the damping effect due to different placements of EDR devices, and this value depends highly on the associated initial conditions and the output matrix of the system. At the same time, it is not reasonable to select the configuration just based on the magnitude of damping coefficient of a specified mode.

B. Design Example

The same truss structure with node numbers as shown in Fig. 1 is used to demonstrate our design idea. The task is to find the placement of 5 EDR devices within the given 13 candidates for the one giving the best damping effect. These candidates are in the truss elements connecting 7→6, 7→1, 7→2, 7→3, 7→8, 8→2, 8→3, 8→4, 8→9, 9→3, 9→4, 9→5, and 9→10. To simplify the design process, we assume that there is always a EDR device located in the truss element connecting node 8→3 (the seventh candidate), and there are four remaining EDR devices to be placed. Hence, this problem is reduced to select the best two locations from the first to sixth candidates due to the symmetry of the truss structure, and only 15 possible cases need to be considered.

A lumped system is considered for modeling the truss structure, in which nodes 7, 8, and 9 located with mass m are applied with control forces, and the corresponding output signals (displacements) are measured, respectively, as shown in Fig. 1. Thus, the corresponding output matrix $\boldsymbol{C}$ has the identity submatrices $\boldsymbol{C}_q$, $\boldsymbol{C}_v$ with dimensions six. The EDR device's parameter k_h is $0.75EA/L$ or $0.75EA/(\sqrt{2})L$ for each truss element of length L or $(\sqrt{2})L$, respectively. The truss structure with 13 EDR devices located at all of the candidates is chosen as a reference for comparison, and this configuration is referred as the complete configuration. The natural frequencies, damping coefficients, and Hankel singular values for the complete configuration are computed and are listed in Table 3.

Because the damping ratio is not considered to be much less than one in this case, the equation of motion is represented as a state-space realization instead of a modal state-space representation. The computational algorithm, presented in Sec. III.B., is used to compute the placement index for each possible combination.

To select a suitable configuration for arbitrary disturbance, various initial conditions given in Table 4 are used for the further analysis. Table 5 lists all placement indices for 15 possible combinations under each set of initial conditions. From these results, it is known that the ordering of the placement indices γ will change when different initial conditions are used. This shows that the best configuration cannot be determined according a specified initial condition. However, we can select the best configuration by using the worst-case placement index $\gamma^* = \sigma_1^2$. The other way is to select a large number of initial conditions to stimulate the environmental uncertainty, such as gust, wind, etc., e.g., we use 1000 randomly generated initial conditions for the demonstrative purpose, and then to take the maximal placement indices γ of these initial conditions.

It is seen clearly from the results of Table 5 that configuration 1 is the best choice. The result for 1000 random initial conditions is similar to the result by the worst-case design rule. This shows that the worst-case design rule does consider many possible initial

Table 3 Natural frequencies, damping ratios and Hankel singular values for complete configuration of design example

Configuration	No	1	2	3	4	5	6
	ω_i	18.78	33.96	36.65	44.16	58.54	63.51
Complete	ζ_i	1.0220	0.3004	0.2115	0.1835	0.1635	0.1634
	$\sigma_i \times 10^2$	0.2904	0.2534	0.1572	0.1458	0.0700	0.0142

Table 4 Different initial conditions for γ testing

γ	Conditions
γ_1	$\boldsymbol{w}(0) = \boldsymbol{0}, \quad \dot{\boldsymbol{w}}(0) = \sum_{i=1}^{6} \varphi_i$ cm/s
γ_2	$\boldsymbol{w}(0) = (\varphi_1 + 0.5\varphi_2 + 0.25\varphi_3 + 0.15\varphi_4 + 0.1\varphi_5 + 0.05\varphi_6)$ cm $\dot{\boldsymbol{w}}(0) = \boldsymbol{0}$
γ_3	$\boldsymbol{w}(0) = \varphi_1$ cm, $\quad \dot{\boldsymbol{w}}(0) = \boldsymbol{0}$
γ_{random}	$\boldsymbol{w}(0), \dot{\boldsymbol{w}}(0)$ are given by random number generator for 1000 times and then γ is obtained by taking their maximum

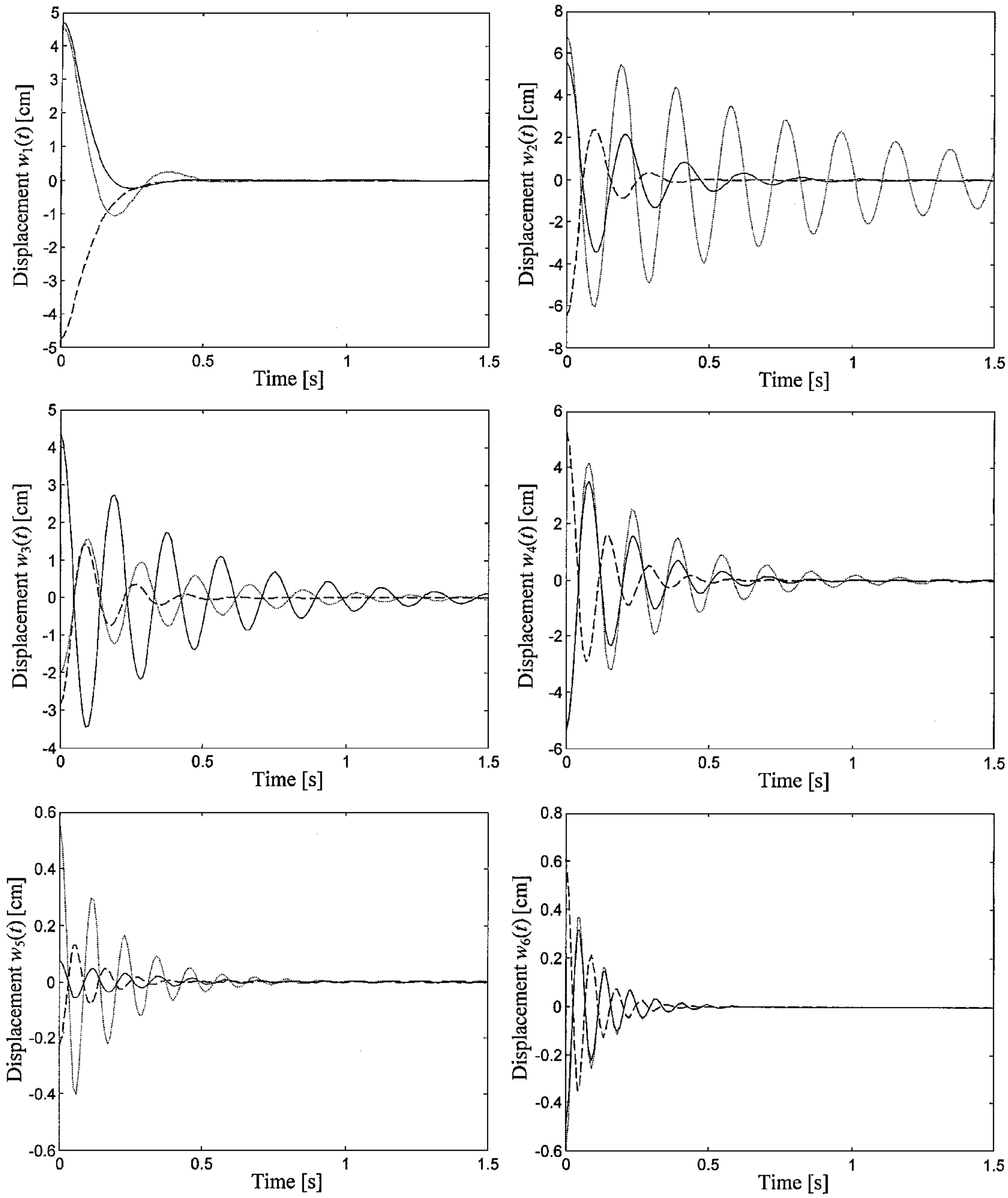

Fig. 3 Time response of displacements $w(t)$: – – –, complete configuration; · · · · ·, configuration 1; and ——, configuration 5.

Table 5 Placement indices ($\times 10^5$) for each configuration under different initial conditions

Configuration	Layout of EDR placements	γ^*	γ_1	γ_2	γ_3	γ_{random}
Complete	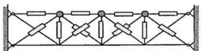	0.8434	1.2782	5.1038	12.435	10.365
1	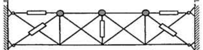	54.330	7.8867	11.700	91.991	53.859
2	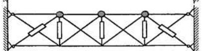	200.0	3.8200	1.5479	34.932	120.00
3	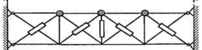	2100.0	44.530	51.929	40.004	160.00
4	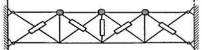	87.870	54.793	44.253	52.896	67.400
5	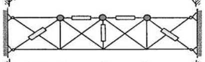	370.0	6.8726	35.542	91.991	110.00
6	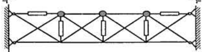	63.670	15.062	20.445	36.014	68.237
7	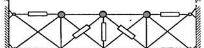	2700.0	21.863	110.00	48.009	390.00
8	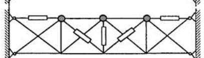	860.0	18.841	81.754	55.452	310.00
9	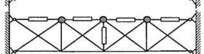	22720.0	6.5624	63.807	130.00	30.000
10	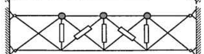	6420.0	180.00	100.00	19.158	1680.00
11	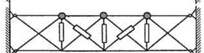	300.0	65.510	25.332	23.333	170.00
12	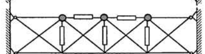	170.0	3.7639	16.321	36.014	59.240
13	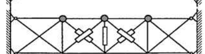	840.00	39.835	89.477	29.701	200.00
14	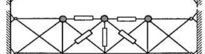	7310.0	6.5858	49.971	48.009	410.00
15	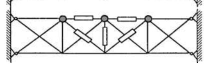	10460.0	4.6313	44.711	64.164	440.00

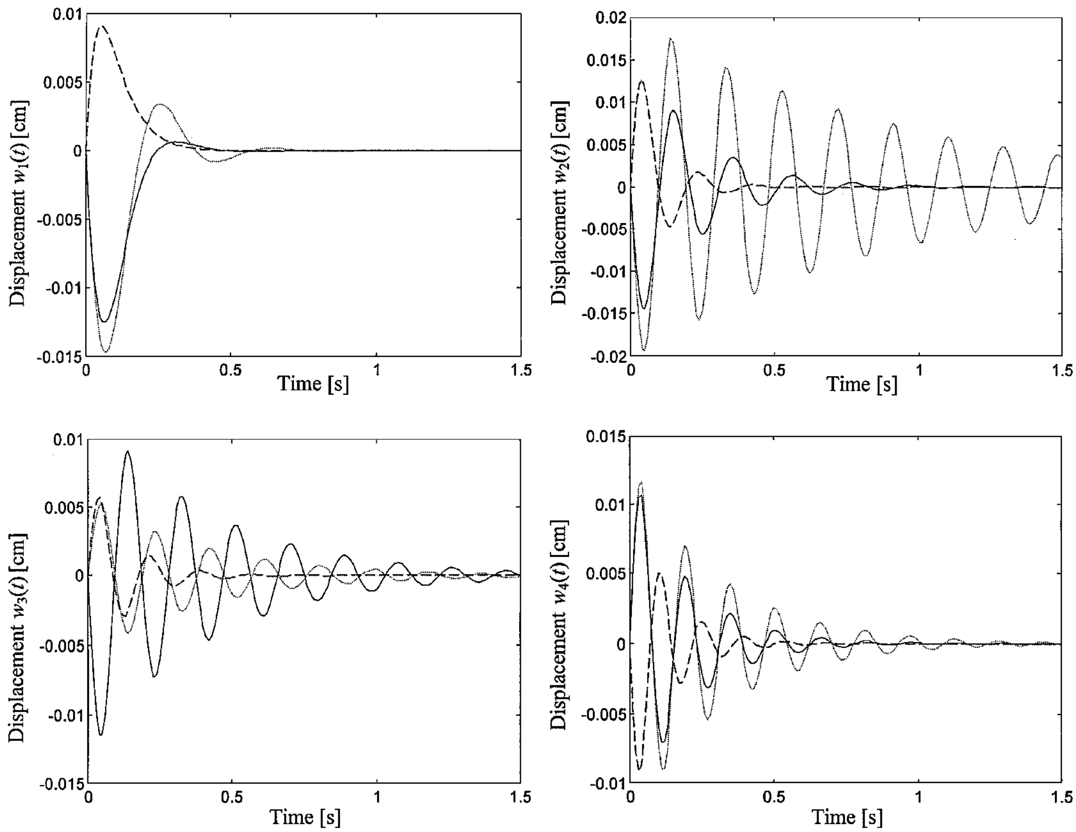

Fig. 4 Time response of displacements $w_1(t)$, $w_2(t)$, $w_3(t)$, and $w_4(t)$ with impulse control force u_1 (others are very small and omitted): – – –, complete configuration; ·····, configuration 1; and ——, configuration 5.

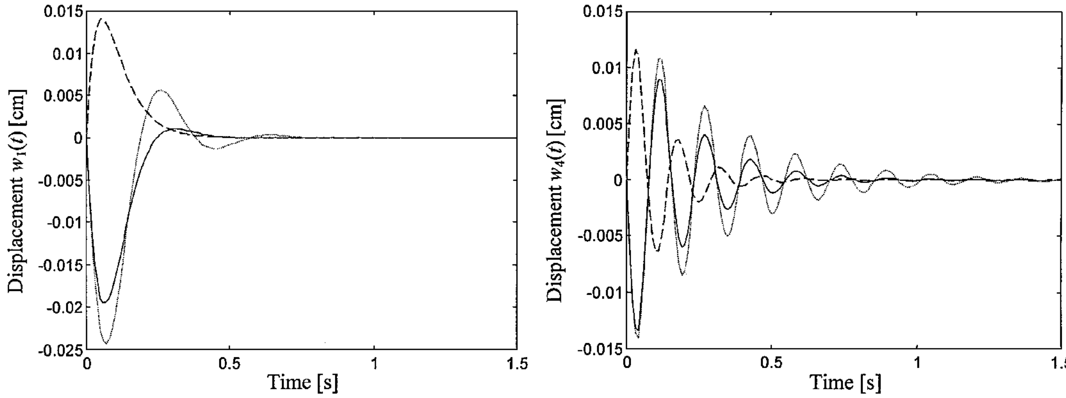

Fig. 5 Time response of displacements $w_1(t)$ and $w_4(t)$ with impulse control force u_2 (others are very small and omitted.): - - -, complete configuration; ·····, configuration 1; and ——, configuration 5.

conditions. To investigate the effect of EDR dissipator on the dynamic response of configuration 1, we choose configuration 5 for comparison and the complete configuration for reference. We know in advance that the dynamic response of the complete configuration is superior to all of the other configurations because since this configuration contains 13 EDRs. Choose the initial condition to be $\boldsymbol{w}(0) = [10, 0, 0, 0, 0, 0]^T$ cm, $\dot{\boldsymbol{w}}(0) = \boldsymbol{0}$, and then compute the time responses of w_1, w_2, w_4, and w_5 corresponding to the complete configuration, configuration 1, and configuration 5, which are shown in Fig. 3. This test shows that configuration 5 is better than the configuration 1, which is consistent to our selection. In addition, we also test the vibration suppression effect of these three different configurations under an impulse control force u_1 or u_2. Their associated time responses of displacements are shown in Figs. 4 and 5, respectively, which indicate that configuration 5 still provides better suppression for vibration, i.e., provides a better damping effect, than configuration 1.

V. Conclusions

A technique for designing optimal placement of linear-friction dissipators for truss structures has been presented. The energy balancing for a linear finite dimensional system has been briefly reviewed. When the square of the damping coefficient of flexible structures is much less than unity, the Hankel singular values can be expressed in terms of the natural frequencies, damping coefficients, and input–output assignments. To date the physical meaning of each Hankel singular value, except the largest one, is unclear; the present result reveals that each Hankel singular value can be directly linked to the modal damping coefficient and natural frequency of flexible structures with small damping. To investigate the placement of EDR devices, we have set up two placement indices for selecting a suitable arrangement of dissipators such that one is used for a fixed initial condition and the other is for all possible initial conditions, i.e., worst-case design. In addition, we have set up a general framework of selecting the dissipators arrangement based on Hankel and H_∞ criteria. To simplify the numerical computation, the harmonic linearization technique is used to model the nonlinear dissipator, and the equation of motion is transformed into state-space representation. For illustration, different dissipator placements of truss structures have been investigated, based on the proposed placement indices. Results show that the placement index is very sensitive to the initial condition and the input–output signal assignments. The larger the placement index, the smaller the damping effect that is produced. Thus, good configurations of EDR device placements for truss structures are those with small placement indices. For structures with small damping effect, the present method is similar to the weighted average of the inverse of the damping ratio. It provides a global damping effect comparison instead of modal-based selection. Therefore, the present technique is a valuable approach for determining optimal damper placement for truss structures.

References

[1]Inaudi, J. A., Nims, D. K., and Kelly, J. M., "Linear Friction Dissipators for Truss Structure," *Smart Structures and Materials, SPIE Proceedings, Vol. 2193, Passive Damping*, edited by Cornor D. Johnson, Society of Photo-Optical Instrumentation Engineers, Orlando, FL, 1994, pp. 213–224.

[2]Zambrano, A., Inaudi, J. A., and Kelly, J. M., "Accuracy of the Modal Strain Energy Method," *Smart Structures and Materials, SPIE Proceedings, Vol. 2193, Passive Damping*, edited by Cornor D. Johnson, Society of Photo-Optical Instrumentation Engineers, Orlando, FL, 1994, pp. 284–295.

[3]Gawronski, W., *Balanced Control of Flexible Structures*, Springer–Verlag, London, 1996, Chap. 3.

[4]Gawronski, W., and Hadaegh, F. Y., "Balanced Input–Output Assignment," *International Journal for Systems Science*, Vol. 24, No. 6, 1993, pp. 1027–1036.

[5]Gawronski, W., and Williams, T., "Model Reduction for Flexible Space Structures," *Journal of Guidance, Control, and Dynamics*, Vol. 14, No. 1, 1991, pp. 8–76.

[6]Gawronski, W., and Lim, K. B., "Balanced Actuator and Sensor Placement for Flexible Structures," *International Journal of Control*, Vol. 65, No. 1, 1996, pp. 131–145.

[7]Gawronski, W., and Juang, J. N., "Model Reduction for Flexible Structures," *Control and Dynamic Systems*, edited by C. T. Leondes, Vol. 36, Academic, CA, 1996, pp. 143–222.

[8]Blelloch, P. A., Mongori, D. L., and Wei, J. D., "Perturbation Analysis of Internal Balancing for Lightly Damped Mechanical Systems with Gyroscopic and Circulatory Forces," *Journal of Guidance, Control, and Dynamics*, Vol. 10, No. 4, 1987, pp. 406–410.

[9]Jonckheere, A., "Principal Component Analysis of Flexible System–Open Loop Case," *IEEE Transactions on Automatic Control*, Vol. 29, No. 12, 1984, pp. 1095–1097.

[10]Skelton, R. E., "Cost Decomposition of Linear Systems with Application to Model Reduction," *International Journal of Control*, Vol. 32, No. 6, 1980, pp. 1031–1055.

[11]Williams, T, "Closed Form Gramians and Model Reduction for Flexible Space Structures," *IEEE Transactions on Automatic Control*, Vol. 35, No. 3, 1990, pp. 379–381.

[12]Wortelboer, P., and van Oostveen, H., "Model Reduction Guided by Hankel Singular Value Intervals," *Selected Topics in Identification, Modeling and Control*, Vol. 1, Delft Univ. Press, Delft, The Netherlands, 1990, pp. 12–26.

[13]Moore, B. C., "Principal Component Analysis in Linear Systems: Controllability, Observability and Model Reduction," *IEEE Transaction on Automatic Control*, Vol. 26, No. 1, 1981, pp. 17–32.

[14]Glover, K., "All Optimal Hankel-Norm Approximations of Linear Multivariable Systems and Their L^∞ Bounds," *International Journal of Control*, Vol. 39, No. 6, 1984, pp. 1115–1193.

[15]Inaudi, J. A., and Kelly, J. M., "On the Linearization of Structures Containing Linear-Friction Energy Dissipating Devices," *Proceedings of Damping '93*, Vol. 2, National Technical Information Service, San Francisco, 1993, pp. FCB-1–FCB-20.